Progress in Physics of Applied Materials 6 (2026), Serial Number 13, 331-341

Semnan University

Progress in Physics of Applied Materials

journal homepage: https://ppam.semnan.ac.ir/

Carbon Ash: From Waste Material to Flexible Paper-Based Pressure Sensor

Dania Dhafer Hameed [a], Ghaiath A. Fadhil [b], Burak Yahya Kadem [a]*

[a] *College of Science, Al-Karkh University for Science, Baghdad, Iraq*
[b] *College of Engineering, Al-Karkh University for Science, Baghdad, Iraq*

ARTICLE INFO

Article history:
Received: 20 February 2026
Revised: 8 May 2026
Accepted: 11 May 2026
Published online: 26 May 2026

Keywords:
Composite;
PVA;
Carbon ash;
Pressure sensor;
Functionalization.

ABSTRACT

Carbon ash waste obtained from an Iraqi factory was converted into poly (vinyl alcohol) (PVA)-based composite materials intended for sensor applications. The carbon ash was ground, sieved through a 0.045 mm mesh, suspended in distilled water, and subsequently sonicated for 3 hours. The material was then dried at 100 °C for 15 min. Surface modification was carried out using acetic acid (S1), hydrochloric acid (S2), and sulfuric acid (S3) prior to embedding the modified carbon ash into the PVA matrix to form polymer composites. FTIR spectra showed absorption bands attributed to oxygen-containing functional groups, which improved the interaction between the polymer and carbon ash, particularly in the S3 sample. Electrical conductivity increased to 15.1 $S \cdot cm^{-1}$ for S3. Hall effect results indicated an increase in both carrier mobility and carrier concentration in the acid-treated composites. Cyclic voltammetry showed that the S3 sample had the most pronounced electrochemical response, consistent with its enhanced chemical and electrical properties. Morphological analysis indicated improved filler dispersion in the acid-treated composites, which exhibited a more uniform microstructure, particularly for S3. The pressure sensors fabricated from these materials demonstrated enhanced electromechanical performance, with S3 achieving the highest sensitivity and good structural stability.

1. Introduction

Flexible strain sensors are extensively studied for wearable electronics, electronic skin, and robotics due to their lightweight structure, bendability, sensitivity, and ease of fabrication [1]. These sensors are used for health monitoring, soft robotics, and enhanced human–machine interaction [2–5]. Their performance relies on the efficient conversion of mechanical deformation or pressure into electrical signals. This performance is strongly influenced by the material composition and processing conditions. Unlike conventional rigid sensors based on metals or metal oxides, polymer-based sensors can easily adapt to natural body motions, such as bending, stretching, and twisting, owing to their flexibility and biocompatibility, which enable smooth integration with the human body as skin-like materials. Such materials can move naturally and comfortably with human skin during everyday activities [6]. A low-cost, flexible sensor that detects strain through piezoresistive, capacitive, and impedance responses can be fabricated using screen printing of carbon black:PVA ink onto cellulose paper [1], its performance has been compared with that of a commercial carbon-ink sensor. The significant growth in the use of flexible electronics, which are often made from materials with slow degradation rates such as plastics, increases electronic waste and raises environmental concerns [7, 8]. Therefore, different natural and eco-friendly alternatives have been investigated for

* Corresponding author.
E-mail address: drburakkadem@gmail.com

Cite this article as:
Hameed, D.D., Fadhil, G.A. and Kadem, B.Y., 2026. Carbon Ash: From Waste Material to Flexible Paper-Based Pressure Sensor. *Progress in Physics of Applied Materials*, *6*(4), pp.331-341. DOI: 10.22075/ppam.2026.40653.1209

wearable electronics applications, such as paper [9], gelatin [10], and silk-based proteins [11].

Among polymer materials, poly (vinyl alcohol) (PVA) is a promising alternative; it exhibits excellent film-forming ability, biocompatibility, mechanical flexibility, and straightforward processability [12]. To further improve PVA-based composites, carbon-based fillers such as carbon ash (CA), a low-cost byproduct of combustion, offer a sustainable solution. However, weak interfacial interactions between untreated carbon ash and the polymer matrix often limit performance improvement. One effective approach to address this issue is chemical functionalization, which enhances filler dispersion, compatibility, and bonding within the polymer matrix [13].

Common acid treatments using acetic acid, hydrochloric acid (HCl), and sulfuric acid (H_2SO_4) introduce oxygen-containing functional groups, such as carboxyl, hydroxyl, and sulfonic groups, onto the carbon surface [14, 15]. These functional groups improve polymer–filler adhesion and enable tuning of the electrical and structural properties of the composite. In this work, carbon ash is utilized because of its attractive structural characteristics and availability as a recyclable industrial waste material. The accumulation of fly carbon ash creates serious disposal challenges, which motivates recycling approaches [16]. The results of this study may provide a new route for recycling fly ash generated in Iraqi industrial factories.

Previous research supports this direction. Several studies have demonstrated the usefulness of PVA-based composites in flexible sensors. Liu et al. [17] evaluated PVA/carbon-based composites in paper electronics and showed that PVA provides adjustable flexibility while carbon fillers enhance the electrical conductivity of the composite. Other studies have reported [18] the fabrication of a paper-based piezoresistive sensor using carbon materials and PVA that remains sensitive even under humid or underwater conditions. Furthermore, Han et al. [19] examined PVA/carbon composites as strain sensors, developing a sensor capable of self-sensing resistance changes under applied strain, which provides useful concepts for paper-based strain sensors. Although carbon-based conductive fillers in PVA matrices have been extensively reported, the present work utilizes industrial carbon ash waste as a low-cost, sustainable, and environmentally beneficial conductive filler, instead of commercially processed carbon nanomaterials. Unlike conventional fillers such as graphene, carbon nanotubes (CNTs), or carbon black, the material used here originates from industrial waste byproducts, thereby promoting the recycling of waste materials in the fabrication of flexible sensors.

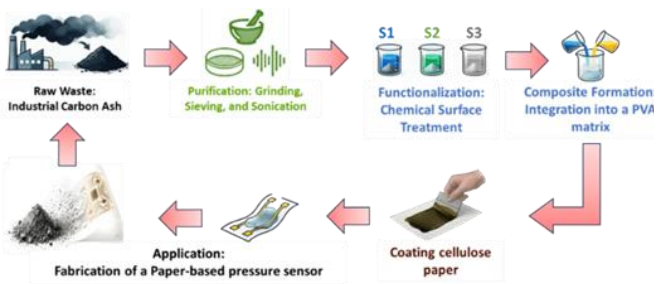

Fig. 1. Chemical transformation of waste ashes into a flexible sensor.

1.1. Sample preparations and properties

A PVA solution was prepared by dissolving 2 g of PVA in 100 mL of distilled water to serve as the matrix material for the composite samples as shown in Figure 1. The PVA solution was stirred at 60 °C for 2 h until a homogeneous, gel-like solution was obtained. The FCA samples (S1, S2, and S3) with a mass of 100 mg were gradually added to 10 mL of the PVA solution and initially mixed manually to prevent agglomeration and improve dispersion. Subsequently, the FCA:PVA mixture was stirred vigorously to achieve a uniform dispersion of FCA within the PVA matrix. Figure 2 illustrates the schematic diagram of the functionalization and dispersion of FCA in the PVA matrix.

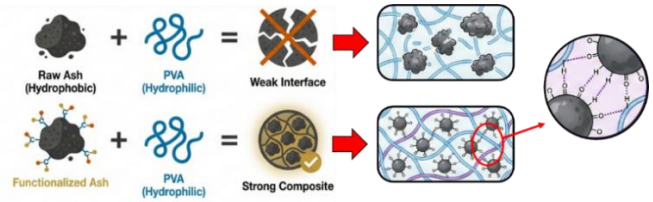

Fig. 2. The functionalization and dispersion of carbon ash within the PVA matrix.

2. Results and Discussions

2.1. FTIR Spectra

To analyze the chemical groups in the FCA:PVA samples, Fourier Transform Infrared (FTIR) Spectroscopy was used as a non-destructive method. The FTIR spectra shown in Figure 3A and the functional groups in Table 1 demonstrate the characteristics of the pure and acid-treated samples. In all samples, a broad band around 3450 cm^{-1} is observed, which is mainly related to the O-H stretching from hydroxyl groups and absorbed moisture. This suggests a strong hydrogen bonding between the PVA-PVA molecules and PVA molecules-CA surface [20]. The alkyl chains related to PVA are observed near 2900 cm^{-1}, which is attributed to the C-H stretching. This band is clearly visible in the pure, S1, and S2 samples but is noticeably weaker in S3. This suggests modifications in the PVA structure and stronger filler interactions. A weak C=O stretching band around 1700 cm^{-1}, typical of PVA vinyl ester groups, is observed in all samples [21]. In addition, bands in the 1400-1450 cm^{-1} range, related to C-H bending vibrations, become stronger in the acid-treated composites, especially S1-S3, indicating structural modification and improved polymer-filler bonding [22]. Bands in the 1250-1360 cm^{-1} are assigned to C-O-C and other PVA-related groups, such as acetyl or ether bonds. The peaks between 1020 and 1120 cm^{-1} are sensitive to PVA crystallinity and related to C=O stretching. This stretching is related to the C-O-C of acetyl groups in PVA [22, 23]. They become noticeably weaker in the S3 sample, which suggests an effective cavity filling within the PVA structure and lowers its crystallinity. This indicates enhanced dispersion and strong crosslinking between PVA and S3 (Fig. 3B) [24]. Notably, the H_2SO_4-treated sample (S3) shows an overall decrease in peak intensity in some regions. This indicates improved carbon surface purification. This is likely to contribute to its enhanced

electrical performance. These changes indicate strong interfacial bonding, mainly through hydrogen bonds between the hydroxyl groups of PVA and oxygen-containing functional groups on the CA surface [25–27]. In addition to surface functionalization, the acid-washing process is also expected to remove residual inorganic impurities and weakly bonded amorphous species from the CA surface. Such purification can expose additional active carbon sites and facilitate stronger interactions with the PVA chains. Therefore, the FTIR changes observed in the treated samples, particularly S3, suggest that acid treatment induces both chemical modification and surface cleaning, which together improve matrix–filler compatibility. Moreover, the bands in the 800–900 cm^{-1} range, usually associated with C–H out-of-plane bending in aromatic structures or related ring vibrations [28].

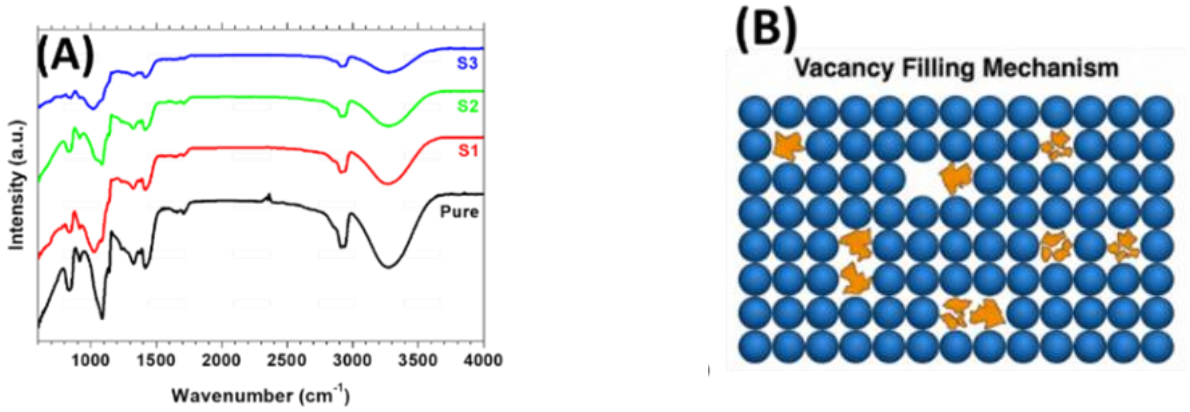

Fig. 3. (A) FTIR spectra of FCA:PVA composites with different functionalization, (B) An illustration of the vacancy filling mechanism to make good cross-linking between the PVA and S3 within the composite.

Table 1. FTIR Peak Assignments for FCA:PVA Composites.

Wavenumber (cm^{-1})	Assignment	Ref
~3450	O–H stretching (hydroxyl, moisture)	[29]
~2900	C–H stretching (alkyl)	[30]
~1700	C=O stretching (vinyl ester)	[31]
~1400-1450	C-H bending and wagging	[32]
~1250-1360	C-O-C (like acetyl in PVA or ether groups)	[32]
~1020-1120	C–O–C stretching (acetyl, PVA crystallinity)	[33]
~800-900	C=C bending (weak bands) and C–H bending	[33]

The FTIR observations indicate that acid treatment not only alter the surface chemistry of CA through the introduction of oxygen-containing groups but also modifies its compatibility with the surrounding PVA chains. The treated samples show stronger matrix-filler interaction, which is expected to reduce local voids and facilitate a more integrated composite structure. Such physiochemical modification is important for constructing stable conductive pathways within the polymer matrix.

2.2. Electrical Conductivity

The electrical conductivity of the composites was examined using current-voltage (I-V) measurements to assess their suitability for electronic and conductive polymer applications. The tests were carried out at room conditions using a Keithley 2400 source meter controlled by LabVIEW. A voltage sweep from -1 V to +1 V was applied to each sample. As shown in Figure 4A, all samples exhibit linear I-V curves, indicating Ohmic behavior and suggesting that charge transport is mainly governed by bulk conduction within the composites. The electrical conductivity was calculated using the following equation [27]:

$$\sigma = {}^{L}/_{AR} \quad (1)$$

Here, σ represents the electrical conductivity, L is the electrode length, A is the electrode cross-sectional area, and R is the material resistance, obtained from the slope of the I-V curve.

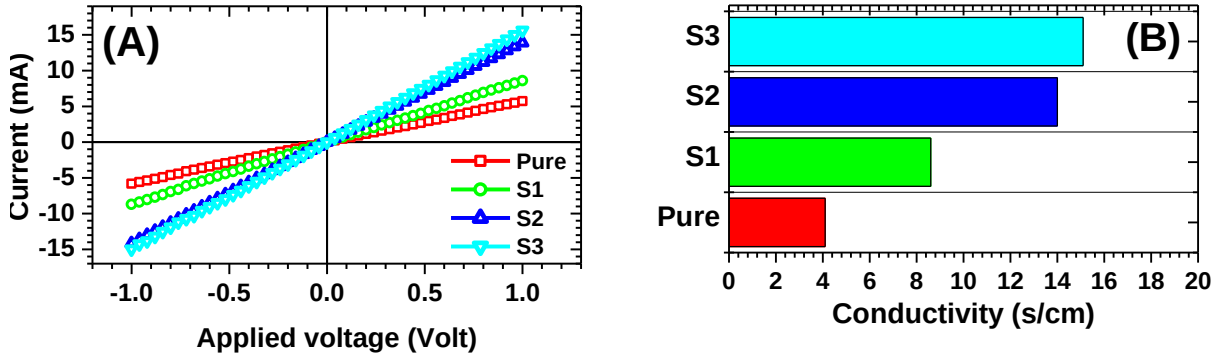

Fig. 4. (A) I-V characteristics and (B) the electrical conductivity of the carbon-based samples.

The results in Figure 4B show a clear increase in conductivity after chemical treatment of the CA. The untreated sample shows the lowest conductivity at 4.1 S/cm. This value increases to 8.6 S/cm for the acetic acid-treated sample (S1) and 14.0 S/cm for the HCl-treated sample (S2). The highest value of 15.1 S/cm was for the sulfuric acid-treated sample (S3). The observed increase in conductivity can be attributed to the combined influence of acid-induced surface chemical modification, elimination of non-conductive impurities, partial structural improvement of the carbon phase, and enhanced interfacial interaction between FCA and the PVA matrix. FTIR results suggest that acid treatment introduces oxygen-containing functional groups capable of forming stronger hydrogen-bond interactions with PVA [34]. In addition, the washing treatment helps purify the carbon surface and reduce particle agglomeration, thereby promoting the formation of more continuous conductive pathways. Notably, the FTIR spectrum of the S3 sample exhibits a significant weakening of the crystallinity-related bands at 1020 and 1120 cm^{-1}, indicating reduced PVA chain ordering and stronger matrix-filler interaction. This behavior is consistent with the more homogeneous filler distribution observed in the morphological analysis and contributes to lower interfacial resistance and more efficient charge transport throughout the composite. Such a result confirms strong hydrogen bonds between the hydroxyl groups of PVA and the oxygen-containing functional groups on the carbon surface [26,35]. Previous studies revealed that the acid-treated carbon surface disrupts the semi-crystalline structure of the polymer by introducing defects and polar groups, which further facilitates electrical conduction [26,35]. The dispersion of FCA within the PVA matrix for enhancing the charge transport pathway has been demonstrated in Figure 5.

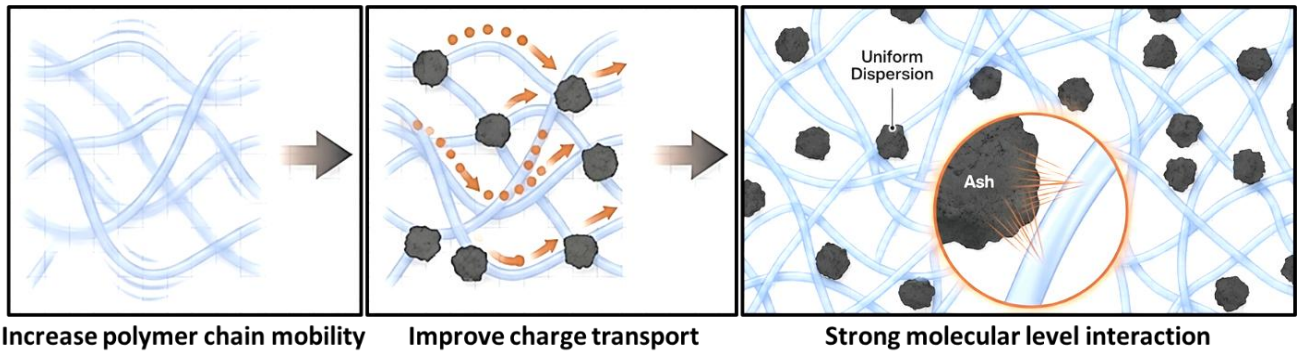

Fig. 5. The dispersion of FCA within the PVA matrix for enhancing the charge transport pathway.

Also, the sulfuric acid treatment partially purified and graphitized the CA by reducing the non-conductive amorphous carbon and increasing sp2-bonded domains, allowing better π-electron delocalization and higher conductivity [27]. As a result, chemical functionalization improves compatibility between the carbon filler and the polymer matrix and strengthens electrical pathways throughout the composite.

2.3. Hall Measurements

The Hall effect measurements were used to investigate charge transport behavior in the studied composites; samples were prepared with the dimensions of 1.2 cm x 1.2 cm. The pure composite shows a measurable electrical conductivity of 8.6 S/cm (Fig. 6A). This is attributed to the weak interfacial interaction between the CA and the PVA matrix due to the lack of surface functional groups, which can facilitate partial conductive pathways formed by the carbon ash particles. This process leads to lower carrier mobility and carrier density (Fig. 6B and 6C).

In contrast, the acid-treated samples exhibited higher values of Hall parameters. The S1 sample (acetic acid-treated) showed a carrier density of 1.04×10^{21} m^{-3} and a mobility of 0.516 $cm^2/V{\cdot}s$, corresponding to a conductivity of 8.6 S/cm. The S2 sample (HCl-treated) displayed higher values, with a carrier density of 1.56×10^{21} m^{-3} and mobility of 0.561 $cm^2/V{\cdot}s$, resulting in a conductivity of 14.0 S/cm. The S3 sample (H_2SO_4-treated) exhibited the highest carrier density of 1.95×10^{21} m^{-3}, mobility of 0.583 $cm^2/V{\cdot}s$, and a maximum conductivity of 15.1 S/cm. These Hall effect results are associated with the overall physicochemical modification of the CA after acid treatment. Besides introducing oxygen-containing functional groups, the treatment removes insulating residues and improves the conductive quality of the carbon particles, while also enhancing their distribution within the PVA matrix. As a result, more continuous low-resistance pathways are formed, reducing carrier scattering and increasing both carrier density and mobility. FTIR analysis confirmed the introduction of oxygen-containing groups, such as hydroxyl and carboxyl groups, after acid treatment. These groups enhance hydrogen bonding with PVA, improving filler dispersion and interfacial adhesion. More continuous and lower-resistance conduction pathways are formed. This enables more efficient charge transport. These insights demonstrate that acid functionalization enhances carrier density, mobility, and conductivity. This supports the suitability of these composites for flexible electronics and electrode applications.

2.4. Cyclic Voltammetry (CV)

Cyclic voltammetry (CV) measurements were performed using a screen-printed carbon electrode purchased from DropSens, Spain. A volume of ~10 µl from the CA:PVA solution was drop-cast onto the working electrode and dried in an oven to remove the solvent and

create a well-adhered, stable film. Potassium chloride (KCl) solution was used as an electrolyte to cover the screen-printed electrodes (working, reference, and counter electrodes) and allow proper electrical contact. Five cycles of CV scans were performed within a potential window of -1 to +1 V at a scan rate of 50 mV s-1. The resulting CV curves shown in Figure 7 are used to estimate the redox behavior and cycling stability of the studied materials.

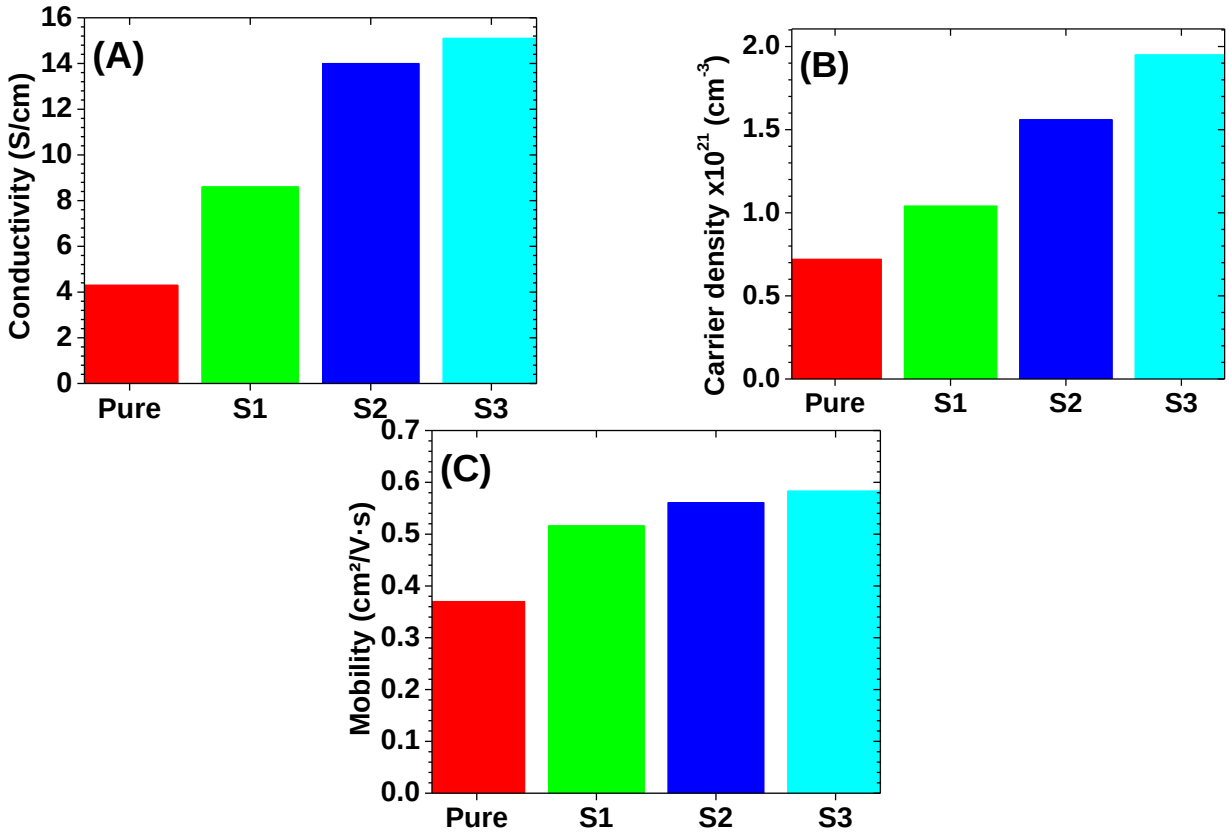

Fig. 6. (A) Conductivity, (B) carrier density and (C) Mobility, of the studied composites.

The S3 (H_2SO_4-treated) shows the strongest electrochemical response among the studied samples, which is characterized by the widest CV loop and observable anodic and cathodic peaks over repeated cycles. Based on the FTIR analysis, the high concentration of surface functional groups (such as -OH and -COOH) introduced by sulfuric acid treatment enhances electrolyte interaction and facilitates faster electron and ion transfer [36]. Therefore, the enlarged CV loop and the increased current response mainly indicate enhanced electrochemical surface conductivity, improved electrolyte accessibility, and more efficient electron/ion transfer at the composite-electrolyte interface. Moreover, it could be claimed that the results in Figure 6 further support the highest CV performance of S3. The sample treated with HCl (S2 sample), the redox activity, the CV loop, and the peak currents are still high and slightly lower compared to the S1 sample. This is also in good agreement with the FTIR results, which confirm the presence of oxygen-containing groups, and with the results of the S2 sample presented in Figure 6. In contrast, the S1 sample (acetic acid-treated) displayed narrower CV loops and the lower current response, which reflects a limited surface functionalization and reduced transport charge, as confirmed by FTIR and Hall measurements.

On the other hand, the untreated sample shows the weakest CV response, with a narrow loop area and low current density, reflecting limited interfacial conductivity and poor electrolyte interaction, which aligns with its low conductivity, carrier mobility, and lack of active surface groups. It should be noted that the observed CV behavior in the present composites is mainly associated with interfacial charge transport and capacitive current response rather than a pronounced faradaic redox storage mechanism.

2.5. The Morphological Properties of Composites

The surface morphology of the composites was examined using scanning electron microscopy (SEM), atomic force microscopy (AFM), and optical imaging; the results are illustrated in Figure 8. These techniques provide a clear observation of the surface morphology and an indication of the FCA dispersion within the PVA matrix, as well as their integration onto the cellulose structure for all samples. For the pure sample, the SEM images reveal a highly irregular and non-uniform surface with clear particle agglomeration, indicating poor dispersion of CA within the PVA matrix and weak interfacial interaction. This behavior is attributed to the lack of polar functional groups, which limits chemical bonding between CA and PVA, as confirmed by FTIR results. This agglomeration is further confirmed by optical and AFM images, which show clustered particles and phase separation within the PVA matrix, resulting in increased surface roughness. The high

surface roughness reflects poor matrix–filler compatibility and the formation of a heterogeneous structure. Such agglomeration weakens the interfacial bonding with the PVA matrix, negatively affecting the mechanical integrity and overall performance of the composite films [37,38].

In contrast, improved dispersion of CA within the PVA matrix is observed in the SEM image of the S1 sample (acetic acid-treated CA), which is mainly due to the introduction of polar carboxyl groups on the CA surface. These groups interact with the hydroxyl groups of PVA, as confirmed by FTIR peaks related to C=O and -OH groups, leading to enhanced electrical performance. For the S2 sample (HCl-treated CA), a more interconnected and compact morphology is observed in the SEM images, suggesting stronger FCA–PVA adhesion due to increased hydrogen bonding via surface -OH groups, as confirmed by FTIR results, and the formation of a more effective percolation network. The S3 sample (H_2SO_4-treated CA) exhibits the most uniform and densely packed structure in SEM images among the samples. The strong oxidizing nature of sulfuric acid introduces a high density of oxygen-containing functional groups and enhances chemical affinity with PVA, which results in excellent dispersion and optimal interfacial contact between the FCA and the PVA matrix.

These results demonstrate that surface functionalization of CA is a critical factor for improving both the structural and electrical properties of PVA-based composites, with H_2SO_4 treatment providing the most effective enhancement. The AFM image of the pure sample confirms the SEM results about the large agglomerates where a rough surface reflecting poor dispersion is observed. The S1 sample shows a reduced surface roughness and smaller surface clusters, indicating better FCA and PVA dispersion and a more homogeneous surface with fewer and smaller aggregates, suggesting stronger interfacial interaction between CA and PVA. Furthermore, the S3 sample exhibits the smoothest surface among the other samples with finely distributed, granular domains and minimal aggregation, confirming excellent dispersion and strong interfacial bonding between filler and matrix [39]. This improved morphology is not only related to the introduction of oxygen-containing surface groups but also to the reduction of particle agglomeration caused by acid-assisted cleaning and separation of CA particles during sonication and centrifugation. The removal of loosely attached impurities and finer redistribution of carbon domains after treatment produce a more homogeneous conductive filler network inside the PVA matrix. These morphological trends directly correlate with the FTIR and electrical results. Furthermore, the optical images of the studied composite (pure, S1, S2, and S3) on the cellulose paper surface show a smooth surface. This is an important finding, as cellulose can be sensitive to acidic environments [40]. The absence of visible degradation indicates that the functionalized composites are mild enough to preserve the cellulose structure, confirming their suitability as flexible substrates for electrical and sensor applications.

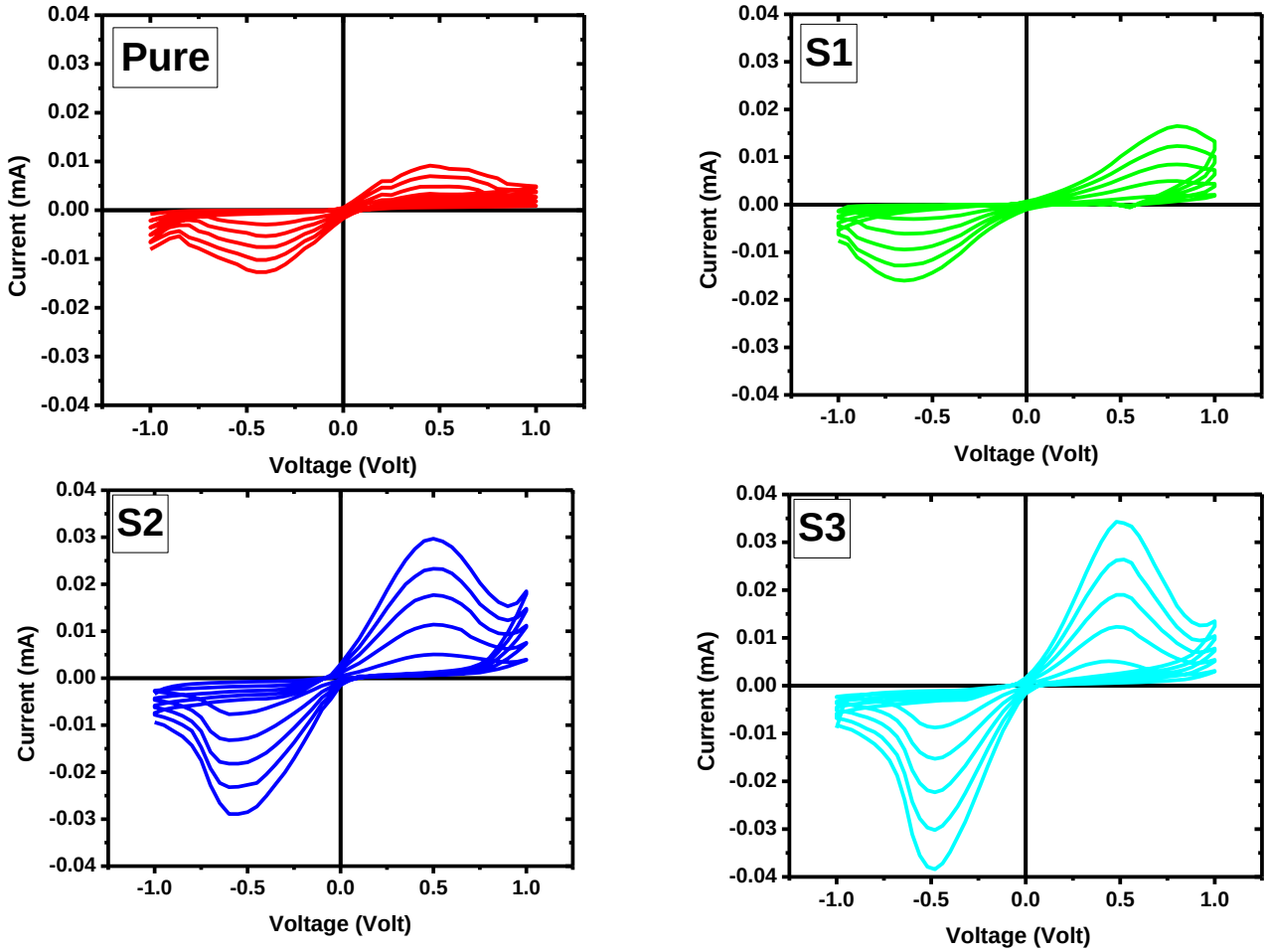

Fig. 7. Cyclic voltammetry scan of the studied composite solutions.

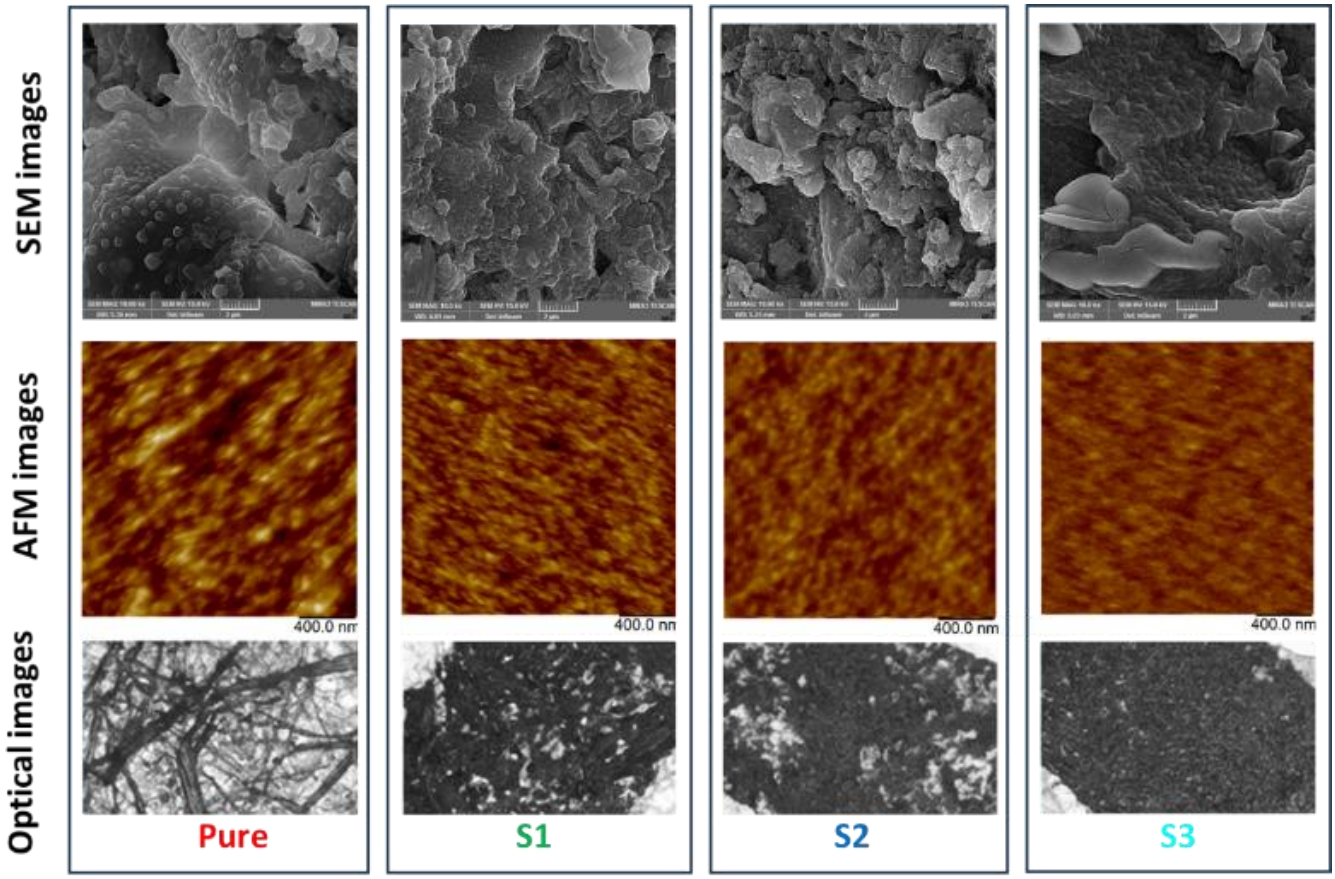

Fig. 8. The morphological properties, including SEM, AFM, and optical images of unfunctionalized PVA: CA (pure) and PVA: FCA composites with different acids (S1) Acetic Acid, (S2) HCl and (S3) H_2SO_4.

2.6. Mechanical Properties (Bulk Modulus)

The bulk modulus (B) of a material measures its resistance to uniform compression. It is defined as the pressure increase needed to decrease the volume [41]. The mechanical properties of the studied samples were analyzed using an ultrasonic measurement described in the literature [41]. The bulk modulus results shown in Figure 9 demonstrates a clear increasing trend from the pure sample to S3 (Fig. 9A) with the pure sample shows the lowest modulus of 5233 MPa, making it the most compressible and flexible sample. The S1 sample shows a slight increase in bulk modulus to 5439 MPa, indicating a small improvement in stiffness while still preserving good flexibility. A more pronounced change is observed in S2, which reaches a bulk modulus of 6723 MPa, with an increase of about 28% compared to the pure sample. This suggests a less compressible material that still retains sufficient flexibility. The S3 sample exhibits the highest bulk modulus of 7219 MPa), making it the stiffest among the studied composites, yet still within the flexible polymer range.

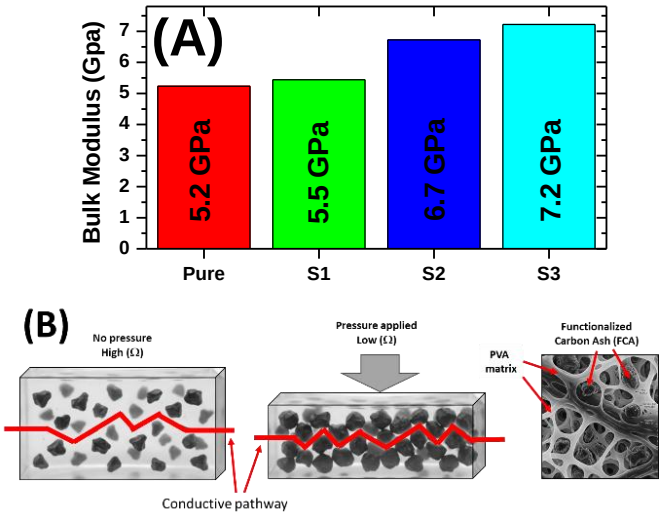

Fig. 9. (A) The bulk modulus for the carbon ash-based composites and (B) An illustration of the FCA:PVA composite before and after pressure showing the conductive pathway and the insight of these composites.

This moderate increase in stiffness is beneficial for flexible sensor applications. The enhanced modulus improves mechanical stability and enables more effective stress transfer to the conductive network. The latter will lead to controlled sample deformation, formation of conductive pathways, improved sensitivity and signal stability under applied pressure. This behavior is attributed to the ability of S3 to effectively fill voids within the PVA matrix and reduce its crystallinity, as demonstrated in Figure 3B. The uniform dispersion of FCA and strong cross-linking within the PVA matrix enhance structural integrity [42]. These effects promote the formation of efficient conductive pathways during compression, leading to a higher sensor response, as shown in Figure 9B.

2.7. Paper-Based Strain Sensor

Our previous work [43] showed that carbon-based fillers in a PVA/PEDOT:PSS matrix have strong pressure-sensing performance. The present FCA:PVA composites are also promising candidates for pressure sensor applications due to their improved structural and electrical properties. The prepared FCA:PVA solutions were coated separately on cellulose paper and allowed to dry overnight before further testing. For practical pressure-sensing applications, several performance indicators must be considered, including sensitivity, response stability, repeatability during loading/unloading, and the ability to generate distinct resistance changes under small external deformations. Therefore, the electrical response of all fabricated sensors was comparatively analyzed under repeated manual pressure cycles. In paper-based pressure sensors, surface uniformity is a key factor, as it directly influences electrical stability, mechanical durability, and overall sensor response. During the electrical sensing measurements, several precautions were taken to minimize signal noise and external fluctuations. All measurements were carried out at room temperature under stable laboratory conditions, and the sensor terminals were fixed firmly using copper clips to ensure constant electrical contact during repeated loading/unloading cycles. The applied pressure was introduced manually in a controlled and consistent manner at nearly the same positions on the sensor surface to reduce mechanical variation. In addition, the baseline resistance of each sample was allowed to stabilize before recording, and the acquired signals were monitored only after transient fluctuations had subsided. Each sensing experiment was repeated at least five times for every sample, and the presented response curves represent reproducible measurements. A smoother surface responds more uniformly to pressure, produces more consistent electrical signals, and withstands repeated loading without damage.

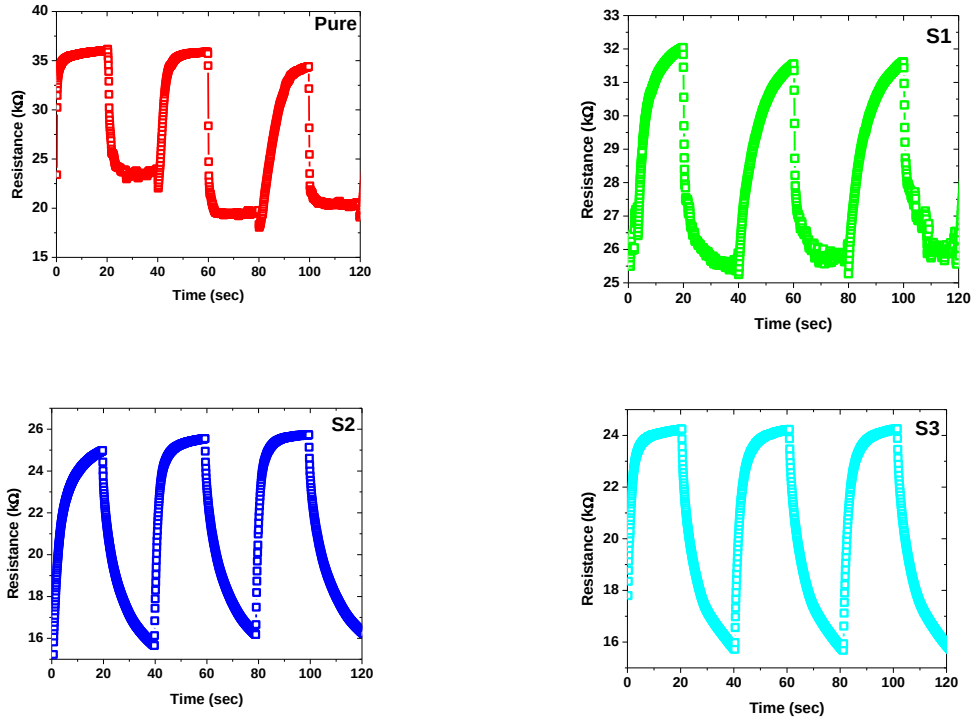

Fig. 10. Pressure sensor response (time vs. resistance) for all the samples under study.

The sensor response curves presented in Figure 10 show the behavior of the PVA:FCA composite films when used as pressure or strain sensors under conditions relevant to medical applications, such as pulse sensing, skin movement, and motion monitoring. As shown in Figure 10, all sensors exhibit a measurable resistance variation under periodic pressure application, confirming their piezoresistive behavior (see Fig. 11). However, the magnitude of resistance change differs significantly among the samples.

The untreated sensor shows only a weak signal fluctuation, indicating low pressure sensitivity due to discontinuous conductive pathways. In contrast, the acid-treated samples produce progressively larger and clearer

resistance responses, suggesting that their sensitivity increases with improved FCA dispersion and conductive-network formation. Among them, the S3 sensor exhibits the highest signal amplitude, indicating the strongest pressure-dependent electrical modulation.

The enhanced sensing performance of the acid-treated composites can be understood as a cumulative result of the earlier physicochemical observations. Acid treatment modifies the CA surface chemistry, removes residual non-conductive impurities, reduces agglomeration, and improves filler dispersion within the PVA matrix. These combined effects promote the formation of a stable conductive network and more efficient resistance variation under external pressure.

The better performance of S3 arises from several factors: its high electrical conductivity, high carrier density, and strong bonding between FCA and PVA due to sulfuric-acid-introduced functional groups, as confirmed by the previous results. Such stable conductive pathways allow pressure signals to be transmitted more efficiently through the material. The S2 and S1 samples show moderate performance, while the untreated sample has the lowest potential for practical sensing applications due to its weak and unstable response.

In addition to sensitivity, response repeatability is an important indicator of the performance of flexible sensing materials. The treated samples, particularly S2 and S3, exhibit relatively consistent peak-to-peak resistance changes over successive loading–unloading cycles with limited baseline drift, indicating stable reconstruction of conductive pathways during repeated compression. This reproducible behavior confirms improved electromechanical stability compared with the untreated composite. The rapid resistance transitions observed during each pressure application and release cycle demonstrate that the developed composites can effectively convert external mechanical deformation into readable electrical signals. Such behavior is essential for low-pressure biomechanical monitoring applications, including finger motion detection, gentle touch sensing, pulse-like pressure monitoring, and surface strain detection. Although the present study focuses on comparative sensor behavior under low manual pressure conditions rather than calibrated force values, the obtained responses clearly demonstrate that the fabricated FCA:PVA films operate effectively in a low-pressure deformation regime relevant to wearable and paper-based flexible sensing applications. Compared with previously reported PVA/carbon-based flexible sensors that rely on commercial conductive fillers such as carbon black, graphene, or carbon nanotubes (CNTs), the present system offers the additional advantage of utilizing low-cost industrial carbon ash (CA) waste while still achieving stable and distinguishable piezoresistive responses. Although the sensing performance remains qualitative at this stage, the developed composite demonstrates strong potential as a sustainable and economical pressure-sensitive material.

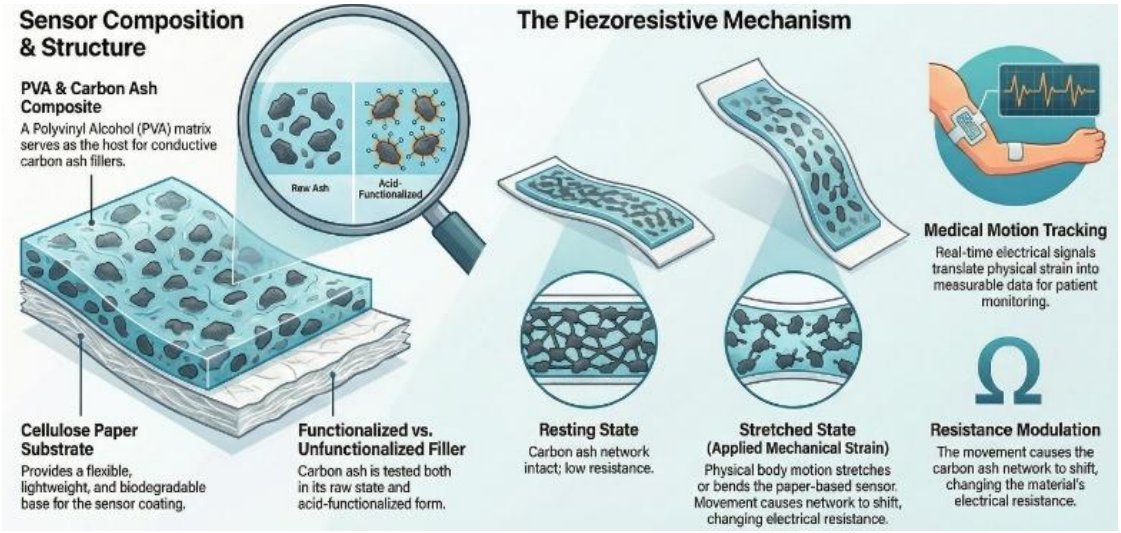

Fig. 11. An illustration of the piezoresistive response of the studied paper-based sensors; this illustration is created by Google Notebook for better demonstration.

3. Conclusions

In this study, PVA-based samples mixed with pure and acid functionalization industrial waste carbon ash was demonstrated to affect the physical, chemical, and electrical properties of these PVA-based composites. The sulfuric acid-treated sample (S3) exhibited better performance among other studied samples with improved FCA dispersion, stronger bonding of FCA with the PVA matrix, higher electrical conductivity, better charge transport, and enhanced electrochemical behavior. FTIR results indicate an introduction of hydrogen bonding between FCA and PVA, which is related to the presence of oxygen-containing functional groups, especially in S3. The morphological properties revealed the effects of different acids functionalization of the CA:PVA-based composites. In addition, these variations in the composite's structure show a direct effect on electrical conductivity where the S3 has demonstrated the highest value; reaching 15.1 S/cm due to higher carrier density and reduced crystallinity. Further measurements, including Hall effect measurements and cyclic voltammetry also verified an

enhancement in the S3 properties compared to the untreated, S1 and S2 samples. These enhancements are linked to its enriched surface chemistry. For the paper-based sensor, the S3-based sensor shows better sensitivity and stability, indicating its suitability for flexible and wearable sensing applications. These findings demonstrate that sulfuric acid functionalization is the most effective approach for improving CA:PVA composites. This offers a sustainable, low-cost pathway for developing high-performance materials for electronic and sensor applications.

Funding Statement

This research received no specific grant from any funding agency.

Conflicts of Interest

The authors declare that they have no known competing financial interests or personal relationships that could have appeared to influence the work reported in this paper.

Authors Contribution Statement

All authors contributed equally to this work.

References

[1] Sekertekin, Y., Bozyel, I. and Gokcen, D., 2020. A flexible and low-cost tactile sensor produced by screen printing of carbon black/PVA composite on cellulose paper. *Sensors*, *20*(10), pp.2908.

[2] Cao, Y., Figueroa, J., Li, W., Chen, Z., Wang, Z.L. and Sepulveda, N., 2019. Understanding the dynamic response in ferroelectret nanogenerators to enable self-powered tactile systems and human-controlled micro-robots. *Nano Energy*, *63*, pp.103852.

[3] Ahmad, J., Andersson, H. and Siden, J., 2019. Screen-Printed Piezoresistive Sensors for Monitoring Pressure Distribution in Wheelchair. *IEEE Sensors Journal*, *19*, pp.2055-2063.

[4] Chi, C., Sun, X., Xue, N., Li, T. and Liu, C., 2018. Recent Progress in Technologies for Tactile Sensors. *Sensors*, *18*, pp.948.

[5] Wan, Y., Wang, Y. and Guo, C.F., 2017. Recent progress on flexible tactile sensors. *Materials Today Physics*, *1*, pp.61-73.

[6] Ajeev, A., Warfle, T., Maslaczynska-Salome, S., Alipoori, S., Duprey, C. and Wujcik, E.K., 2025. From the synthesis of wearable polymer sensors to their potential for reuse and ultimate fate. *Chemical Science*, *16*(21), pp.9056-9075.

[7] Xu, Y., Fei, Q., Page, M., Zhao, G., Ling, Y., Stoll, S.B. and Yan, Z., 2021. Paper-based wearable electronics. *iScience*, *24*, pp.102736.

[8] Su, Z., Yang, Y., Huang, Q., Chen, R., Ge, W., Fang, Z., Huang, F. and Wang, X., 2022. Designed biomass materials for "green" electronics: A review of materials, fabrications, devices, and perspectives. *Progress in Materials Science*, *125*, pp.100917.

[9] Xu, Y., Zhao, G., Zhu, L., Fei, Q., Zhang, Z., Chen, Z., An, F., Chen, Y., Ling, Y., Guo, P., Ding, S., Huang, G., Chen, P., Cao, Q. and Yan, Z., 2022. Pencil-paper on-skin electronics. *Proceedings of the National Academy of Sciences U. S. A.*, *117*, pp.18292-18301.

[10] Sun, Q., Wang, L., Yue, X., Zhang, L., Ren, G., Li, D., Wang, H., Han, Y., Lulu, X., Lu, G., Yu, H.D. and Huang, W., 2021. Fully sustainable and high-performance fish gelatin-based triboelectric nanogenerator for wearable movement sensing and human-machine interaction. *Nano Energy*, *89*, pp.106329.

[11] Li, S., Liu, G., Wen, H., Liu, G., Wang, H., Ye, M., Yang, Y., Guo, W. and Liu, Y., 2022. A skin-like pressure-and vibration-sensitive tactile sensor based on polyacrylamide/silk fibroin elastomer. *Advanced Functional Materials*, *32*(19), pp.2111747.

[12] Kadem, B.Y., 2025. AP0950 Structural, Morphological and Electrical Properties of SiC: PVA: PEDOT: PSS Paper-Based Materials for Flexible Strain Sensors. *Iraqi Journal of Applied Physics*, *21*(4), pp.520-527.

[13] Hussain, F., M. Hojjati, M. Okamoto and Gorga, R.E., 2006. Review article: Polymer-matrix nanocomposites, processing, manufacturing, and application: An overview. *Journal of Composite Materials*, *40*(17), pp.1511–1575.

[14] Dong, C., Campell, A.S., Eldawud, R., Perhinschi, G., Rojanasakul, Y. and Dinu, C.Z., 2013. Effects of acid treatment on structure, properties and biocompatibility of carbon nanotubes. *Applied Surface Science*, *264*, pp.261-268.

[15] Goh, P.S., Wong, K.C., Yogarathinam, L.T., Ismail, A.F., Abdullah, M.S. and Ng, B.C., 2020. Surface modifications of nanofillers for carbon dioxide separation nanocomposite membrane. *Symmetry*, *12*(7), pp.1102.

[16] Temuujin, J. and Van Riessen, A., 2009. Effect of fly ash preliminary calcination on the properties of geopolymer. *Journal of Hazardous Materials*, *164*, pp.634–639.

[17] Liu, E., Cai, Z., Ye, Y., Zhou, M., Liao, H. and Yi, Y., 2023. An overview of flexible sensors: Development, application, and challenges. *Sensors*, *23*(2), pp.817.

[18] Wei, Y., Shi, X., Yao, Z., Zhi, J., Hu, L., Yan, R. and Shi, C., 2023. Fully paper-integrated hydrophobic and air permeable piezoresistive sensors. *npj Flexible Electronics*, *7*, pp.244.

[19] Han, J., Pan, J. and Cai, J., 2022. Self-sensing properties and piezoresistive effect of high ductility cementitious composite. *Construction and Building Materials*, *319*, pp.126055.

[20] Bao, Y., Huang, X., Xu, J. and Cui, S., 2021. Effect of intramolecular hydrogen bonds on the single-chain elasticity of poly (vinyl alcohol): Evidencing the synergistic enhancement effect at the single-molecule level. *Macromolecules*, *54*(15), pp.7314-7320.

[21] Sadiq, M., Khan, M.A., Hasan Raza, M.M., Aalam, S.M., Zulfequar, M. and Ali, J., 2022. Enhancement of electrochemical stability window and electrical properties of CNT-Based PVA–PEG polymer blend composites. *ACS Omega*, *7*(44), pp.40116-40131.

[22] Pranav, C.M., Madhu, G.M., Koteswararao, J. and Kottam, N., 2020. Mechanical and electrical properties evaluation of PVA-carbon dot polymer nanocomposites. *Indian Journal of Chemical Technology*, *27*(6), pp.492-498.

[23] Allayarov, S.R., Confer, M.P., Dixon, D.A., Rudneva, T.N., Kalinin, L.A., Tolstopyatov, E.M., Frolov, I.A., Ivanov, L.F., Grakovich, P.N. and Golodkov, O.N., 2020. Effect of initial γ-irradiation on infrared laser ablation of poly (vinyl alcohol) studied by infrared spectroscopy. *Polymer Degradation and Stability*, *181*, pp.109331.

[24] Hakuto, N., Saito, K., Kirihara, M. and Kotsuchibashi, Y., 2020. Preparation of cross-linked poly(vinyl alcohol) films from copolymers with benzoxaborole and carboxylic acid

groups, and their degradability in an oxidizing environment. *Polymer Chemistry*, *11* (14), pp.2469–2474.

[25] Azhagapillai, P., Al Shoaibi, A. and Chandrasekar, S., 2021. Surface functionalization methodologies on activated carbons and their benzene adsorption. *Carbon Letters*, *31*(3), pp.419-426.

[26] Putro, P.A., Yudasari, N., Isnaeni, I. and Maddu, A., 2021. Spectroscopy study of polyvinyl alcohol/carbon dots composite films. *Walailak Journal of Science and Technology*, *18*(7), pp.9184.

[27] Kadem, B., Cranton, W. and Hassan, A., 2015. Metal salt modified PEDOT: PSS as anode buffer layer and its effect on power conversion efficiency of organic solar cells. *Organic Electronics*, *24*, pp.73–79.

[28] Al-Khafaji, R.S.A., 2021. Synthesis of blend polymer (PVA/PANI)/Copper (1) oxide nanocomposite: thermal analysis and UV-Vis spectra specifications. *Iraqi Journal of Science*, *62*(11), pp.3888-3900.

[29] Alghunaim, N.S., 2016. Optimization and spectroscopic studies on carbon nanotubes/PVA nanocomposites. *Results in Physics*, *6*, pp.456-460.

[30] Ahmad, J., Deshmukh, K. and Hägg, M.B., 2013. Influence of TiO_2 on the chemical, mechanical, and gas separation properties of polyvinyl alcohol-titanium dioxide (PVA-TiO_2) nanocomposite membranes. *International Journal of Polymer Analysis and Characterization*, *18*(4), pp.287-296.

[31] Ahmad, J., Deshmukh, K., Habib, M. and Hägg, M.B., 2014. Influence of TiO2 nanoparticles on the morphological, thermal and solution properties of PVA/TiO_2 nanocomposite membranes. *Arabian Journal for Science and Engineering*, *39*(10), pp.6805-6814.

[32] Mohanapriya, M.K., Deshmukh, K., Chidambaram, K., Ahamed, M.B., Sadasivuni, K.K., Ponnamma, D., AlMaadeed, M.A.A., Deshmukh, R.R. and Pasha, S.K., 2017. Polyvinyl alcohol (PVA)/polystyrene sulfonic acid (PSSA)/carbon black nanocomposite for flexible energy storage device applications. *Journal of Materials Science: Materials in Electronics*, *28*(8), pp.6099-6111.

[33] Pawde, S.M., Deshmukh, K. and Parab, S., 2008. Preparation and characterization of poly (vinyl alcohol) and gelatin blend films. *Journal of Applied Polymer Science*, *109*(2), pp.1328-1337.

[34] Cheong, J.Y., Koay, J.S.C., Gopal, S.R., Velayutham, T.S. and Gan, W.C., 2025. Enhancing the tribopositive characteristics of polyvinyl alcohol (PVA)-carbon composites by optimizing the PVA-carbon interaction with various carbon fillers. *Nanoscale Advances*, *7*(3), pp.819-829.

[35] Hu, M., Gu, X., Hu, Y., Deng, Y. and Wang, C., 2016. PVA/carbon dot nanocomposite hydrogels for simple introduction of Ag nanoparticles with enhanced antibacterial activity. *Macromolecular Materials and Engineering*, *301*(11), pp.1352-1362.

[36] Lee, M. and Park, J.S., 2024. Enhanced performance and durability of pore-filling membranes for anion exchange membrane water electrolysis. *Membranes*, *14*(12), pp.269.

[37] Bantu, T.R., Tom, R.T., Sebasian, D.P. and Kumar, A.C., 2025. Mechanical and Morphological Enhancement of PVA Composites using Crotalaria pallida Fibers. *Malaysian Journal of Chemistry*, *27*(4), pp.207-217.

[38] Suganthi, S., Vignesh, S., Kalyana Sundar, J. and Raj, V., 2020. Fabrication of PVA polymer films with improved antibacterial activity by fine-tuning via organic acids for food packaging applications. *Applied Water Science*, *10* (4), pp.1-11.

[39] Rahman, M.M., Khan, K.H., Parvez, M.M.H., Irizarry, N. and Uddin, M.N., 2025. Polymer nanocomposites with optimized nanoparticle dispersion and enhanced functionalities for industrial applications. *Processes*, *13*(4), pp.994.

[40] Hadhy, R.A. and Kadem, B.Y., 2019. Gel Polymer Electrolyte Based on SiC: PVA Composites for Body motion Sensor and Paper Based Application. In *2019 12th International Conference on Developments in eSystems Engineering (DeSE)*, pp.730-735.

[41] Al-Bermany, E., Qais, D. and Al-Rubaye, S., 2019. Graphene effect on the mechanical properties of poly (ethylene oxide)/graphene oxide nanocomposites using ultrasound technique. *Journal of Physics: Conference Series*, *1234*(1), pp.012011.

[42] Abed, T.H., Abed, M.M., Kadem, B.Y. and Jaiad, A.T., 2021. Rechargeable flexible paper battery using PAV, PSSPEDOT polymer. *IOP Conference Series: Earth and Environmental Science*, *877*(1), pp.012037.

[43] Katagiri, T., Kodama, S., Kawahara, K., Umemoto, K., Miyoshi, T. and Nakayama, T., 2024. Response Characteristics of Pressure-Sensitive Conductive Elastomer Sensors Using OFC Electrode with Triangular Wave Concavo-Convex Surfaces. *Sensors*, *24*(7), pp.2349.